Hyperbolic subdiffusive impedance



2009 J. Phys. A: Math. Theor. 42 055004

(http://iopscience.iop.org/1751-8121/42/5/055004)

IOP PUBLISHING JOURNAL OF PHYSICS A: MATHEMATICAL AND THEORETICAL

J. Phys. A: Math. Theor. **42** (2009) 055004 (14pp) doi:10.1088/1751-8113/42/5/055004

# Hyperbolic subdiffusive impedance

**Tadeusz Kosztołowicz**[1] **and Katarzyna D Lewandowska**[2]

[1] Institute of Physics, Jan Kochanowski University, ul. Świetokrzyska 15, 25-406 Kielce, Poland
[2] Department of Radiological Informatics and Statistics, Medical University of Gdańsk, ul. Tuwima 15, 80-210 Gdańsk, Poland

E-mail: tkoszt@pu.kielce.pl and kale@amg.gda.pl

Received 15 July 2008, in final form 18 November 2008
Published 6 January 2009
Online at stacks.iop.org/JPhysA/42/055004

**Abstract**

We use two different hyperbolic subdiffusion equations with fractional time derivatives (the generalized Cattaneo equations) to study the transport process of electrolytes in media where subdiffusion occurs. In these models the flux is delayed in a non-zero time with respect to the concentration gradient. In particular, we obtain the formulae of electrochemical subdiffusive impedance of a spatially limited sample in the limit of large and small pulsation of the electric field. The boundary conditions at the external wall of the sample are taken in the general form as a linear combination of the subdiffusive flux and the concentration of transported particles. We also discuss the influence of the equation parameters (the subdiffusion parameter and the delay time) on the Nyquist impedance plots.

PACS numbers: 02.90.+p, 05.60.−k

## 1. Introduction

Subdiffusion occurs in systems where mobility of particles is significantly hindered due to internal structure of the medium, as in porous media, gels or amorphous semiconductors [1, 2]. The subdiffusion is characterized by a time dependence of the mean square displacement of a transported particle $\langle \Delta x^2 \rangle = 2D_\alpha t^\alpha / \Gamma(1+\alpha)$, where $D_\alpha$ is the subdiffusion coefficient measured in the units $m^2/s^\alpha$ and $\alpha$ is the subdiffusion parameter of a value within the range $0 < \alpha < 1$. For $\alpha = 1$ one deals with the normal diffusion.

The subdiffusion has been recently extensively studied. While the phenomenon is theoretically rather well understood, there are very few reported experimental investigations (e.g. [1–8]). The method of impedance spectroscopy was used to experimentally study transport in porous media such as nanopore electrode [3], cement [4–6], tooth enamel [7] and

  

gels [8]. The theoretical analysis of subdiffusion impedance was presented by [9] who used the following parabolic subdiffusion equation with fractional time derivative:

$$\frac{\partial C(x,t)}{\partial t} = D_\alpha \frac{\partial^{1-\alpha}}{\partial t^{1-\alpha}} \frac{\partial^2 C(x,t)}{\partial x^2}, \tag{1}$$

where the Riemann–Liouville fractional time derivative is defined for $\alpha > 0$ as [10, 11]

$$\frac{\partial^\alpha f(t)}{\partial t^\alpha} = \frac{1}{\Gamma(n-\alpha)} \frac{\partial^n}{\partial t^n} \int_0^t \mathrm{d}t' \frac{f(t')}{(t-t')^{1+\alpha-n}},$$

and the integer number $n$ fulfils the relation $n-1 < \alpha \leqslant n$. For $\alpha = 1$, equation (1) converts into the normal diffusion equation.

For the initial condition $C(x,0) = \delta(x)$, where $\delta$ is the Dirac-delta function, the solution of equation (1) (the Green's function) has non-zero values for any $x$ and $t$ ($t > 0$). Thus, even for small times, a finite amount of the substance exists at very large distances from the origin, what can be interpreted as the infinite propagation velocity of some of the diffusing particles. To avoid this 'unphysical property' Cattaneo derived the hyperbolic normal diffusion equation for which Green's function has non-zero values for finite $x$ [12, 13]. The equation is based on the assumption that the flux is delayed by time period $\tau$ with respect to the concentration gradient. For many 'typical systems' (as the membrane one) it is hard to observe the difference between the solutions of parabolic and hyperbolic (sub)diffusion equations even for relatively large values of $\tau$ [14]. However, in some processes the non-zero parameter $\tau$ plays a crucial role. The example is the diffusion in a system where boundary conditions are given by functions quickly changing in time. Such a situation occurs in the electrochemical system with (sub)diffusion impedance. As far as we know, the Cattaneo equation was used to study electrochemical impedance only for a system where normal diffusion occurs [15, 16], except our work [17] where the subdiffusion impedance was considered in a system with fully absorbing wall. Articles published so far mostly concentrated on homogeneous systems, however, a more complex system containing few diffusion layers was also studied in [18].

In this paper we present a theoretical foundation for studies of the subdiffusion impedance using a hyperbolic equation. We apply two different hyperbolic Cattaneo equations with the fractional time derivatives to model the subdiffusion impedance of a homogeneous sample of finite thickness, where the boundary condition at the sample surface is assumed as a linear combination of flux and concentration. We find an influence of the parameters $\alpha$ and $\tau$ on the final formula describing the impedance of the subdiffusive medium, particularly for high and for low ac-voltage frequency. We also briefly discuss the properties of the hyperbolic Cattaneo equations which we use.

## 2. The generalized Cattaneo equation

The phenomenological derivation of the Cattaneo equation in the case of normal diffusion is based on the assumption that the flux of the particles $J$ is given by the following formula:

$$J(x,t) + \tau \frac{\partial J(x,t)}{\partial t} = -D \frac{\partial C(x,t)}{\partial x}, \tag{2}$$

with a positive parameter $\tau$. The case of $\tau = 0$ corresponds to the classical Fick law. Combining (2) with the continuity equation

$$\frac{\partial C(x,t)}{\partial t} = -\frac{\partial J(x,t)}{\partial x}, \tag{3}$$

one obtains the hyperbolic normal diffusion

$$\frac{\partial C(x,t)}{\partial t} + \tau \frac{\partial^2 C(x,t)}{\partial t^2} = D \frac{\partial^2 C(x,t)}{\partial x^2}. \tag{4}$$

Equation (2) can be treated as an approximation of the following equation in the limit of small $\tau$:

$$J(x, t+\tau) = -D\frac{\partial C(x,t)}{\partial x}.$$

Thus, the hyperbolic subdiffusion can be interpreted as a process where the flux $J$ is not generated by the concentration gradient instantaneously (as in the process described by the parabolic diffusion equation), but it is delayed in time by $\tau$ [12], what provides the finite propagation velocity of the particles $v = \sqrt{D/\tau}$.

The phenomenological derivation of the hyperbolic subdiffusion equation is often performed by introducing the time derivative of the fractional order into (4). This procedure leads to different hyperbolic subdiffusion equations which are not equivalent to one another. Such a procedure should be treated as a mathematical trick only unless the physical model whereby the subdiffusion equation can be obtained is found. In [13] two different hyperbolic subdiffusion equations which have clear physical interpretation were proposed. In the following we use both of them to model the subdiffusive impedance process. The first model (in the following denoted as 'model A') utilizes the equation

$$\tau\frac{\partial^2 C(x,t)}{\partial t^2} + \frac{\partial C(x,t)}{\partial t} = D_\alpha \frac{\partial^{1-\alpha}}{\partial t^{1-\alpha}}\frac{\partial^2 C(x,t)}{\partial x^2}. \tag{5}$$

In order to find the physical interpretation of equation (5) we go back to the parabolic subdiffusion equation (1). This equation can be derived from the continuous time random walk formalism where the random walk of a transported particle is considered. Its walk is characterized by the distribution of step lengths $\lambda(x)$ and the distribution of waiting times to take the next step $\varphi(t)$. To obtain the subdiffusion equation one assumes that $\lambda(x)$ has a finite dispersion $\sigma$ whereas $\varphi(t)$ provides an infinite mean value. (1) can be also obtained in a phenomenological way by setting the subdiffusive flux

$$J(x,t) = -D_\alpha \frac{\partial^{1-\alpha}}{\partial t^{1-\alpha}}\frac{\partial C(x,t)}{\partial x} \tag{6}$$

to the continuity equation (3). Let us note that the presence of fractional derivative in (5) and (6) is physically well motivated [1]. To obtain the hyperbolic subdiffusion equation, similar as for the normal diffusion case, one assumes that the flux is delayed in time by $\tau$

$$J(x,t+\tau) = -D_\alpha \frac{\partial^{1-\alpha}}{\partial t^{1-\alpha}}\frac{\partial C(x,t)}{\partial x}. \tag{7}$$

Assuming that $\tau \ll t$ and keeping linear terms with respect to $\tau$ in the series expansion of left-hand side of (7), we get

$$J(x,t) + \tau\frac{\partial J(x,t)}{\partial t} = -D_\alpha \frac{\partial^{1-\alpha}}{\partial t^{1-\alpha}}\frac{\partial C(x,t)}{\partial x}. \tag{8}$$

Combining (8) with the continuity equation (3), one obtains the generalized Cattaneo equation (5). Let us note that in this model the parameters $D_\alpha$ and $\tau$ are treated as independent of each other. The parabolic subdiffusion equation can be obtained by putting $\tau = 0$ in (5).

The second hyperbolic subdiffusion equation (which in our paper is used in 'model B') presented in [13] is

$$\frac{\partial C(x,t)}{\partial t} + \tau^\alpha \frac{\partial^{1+\alpha} C(x,t)}{\partial t^{1+\alpha}} = D_\alpha \frac{\partial^{1-\alpha}}{\partial t^{1-\alpha}}\frac{\partial^2 C(x,t)}{\partial x^2}. \tag{9}$$

Equation (9) can be derived within the continuous time random walk scheme, where the flux is given in terms of Laplace and Fourier transforms as [13]

$$\hat{J}(k,s) = -2\mathrm{i}\ell\frac{s}{1-\varphi(s)}\hat{C}(k,s)\int_0^\infty \mathrm{d}x\, \hat{\psi}(x,s)\sin(kx),$$

where $\psi(x,t)$ is the distribution of step lengths and waiting times between steps and $\ell$ is a microscopic length scale necessary to obtain the correct dimension for the flux. In our paper we denote the Fourier transform by $\mathcal{F}\{f(x)\} = \int_{-\infty}^{\infty} \mathrm{e}^{\mathrm{i}kx} f(x)\,\mathrm{d}x = \hat{f}(k)$ and the Laplace one by $\mathcal{L}\{g(t)\} = \int_0^{\infty} \mathrm{e}^{-sx} g(t)\,\mathrm{d}t = \hat{g}(s)$. Assuming that

$$\psi(x,t) = \frac{1}{\sqrt{4\sigma^2\pi}} \exp\left(-\frac{x^2}{4\sigma^2}\right) \varphi(t),$$

where $\varphi(t)$ is defined by its Laplace transform

$$\hat{\varphi}(s) = \mathrm{e}^{-\theta^\alpha s^\alpha},$$

(its inverse Laplace transform in the long time limit reads $\varphi(t) = \theta^\alpha / t^{1+\alpha}\Gamma(-\alpha)$), the following formula:

$$\frac{\mathrm{e}^{s^\alpha\theta^\alpha} - 1}{s^\alpha\theta^\alpha} \hat{J}(k,s) = -\mathrm{i}kD_\alpha s^{1-\alpha} \hat{C}(k,s) \tag{10}$$

was derived in the limit of small $k$ and $s$ [13], where the subdiffusion coefficient is defined as

$$D_\alpha = \frac{\sigma^2}{\theta^\alpha}. \tag{11}$$

Putting

$$\mathrm{e}^{s^\alpha\theta^\alpha} \approx 1 + s^\alpha\theta^\alpha + \frac{s^{2\alpha}\theta^{2\alpha}}{2} \tag{12}$$

into (10) and using the formula $\mathcal{L}^{-1}(s^\alpha \hat{g}(s)) = \partial^\alpha g(t)/\partial t^\alpha$ $(0 < \alpha < 1)$ one gets

$$J(x,t) + \tau^\alpha \frac{\partial^\alpha J(x,t)}{\partial t^\alpha} = -D_\alpha \frac{\partial^{1-\alpha}}{\partial t^{1-\alpha}} \frac{\partial C(x,t)}{\partial x}, \tag{13}$$

where

$$\tau = \frac{\theta}{2^{1/\alpha}}. \tag{14}$$

Combining (13) with the continuity equation (3) one obtains (9). From (11) and (14) we see that the subdiffusion coefficient $D_\alpha$ is controlled by the parameter $\tau$ and reads

$$D_\alpha = \frac{\sigma^2}{2\tau^\alpha}. \tag{15}$$

We find the difficulties in the interpretation of equation (9). The parabolic subdiffusion equation can be obtained from the hyperbolic one by putting $\tau = 0$ in (9). On the other hand vanishing of $\tau$ provides the infinite speed of propagation as it should be. However, due to (15), for $\tau = 0$ one gets the infinite value of the subdiffusion coefficient. We note that the only way to obtain the parabolic subdiffusion equation within this model is to neglect the last term in right–hand side of (12). Then, we obtain the parabolic subdiffusion equation (with the infinite speed of propagation) under the condition that $\tau$ is finite. Despite the objections concerning (9) in the following we apply both equations (5) and (9) to describe the subdiffusion in the system under consideration.

## 3. The system

Let us assume that at $x = 0$ there is the oscillating overvoltage $\eta(t) = E\sin(\omega t)$ which causes the oscillation of the concentration on the surface layer according to the formula

$$\eta|_{x=0}(t) = \left(\frac{\mathrm{d}\eta}{\mathrm{d}C}\right)_{eq} C(0,t), \tag{16}$$

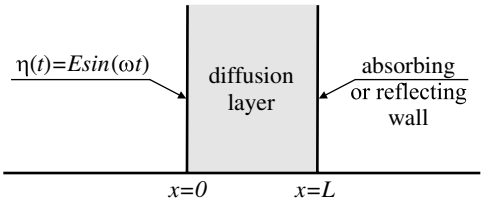


**Figure 1.** The system under considerations, $\eta$ denotes the overvoltage, $E$—its amplitude.

where $eq$ denotes a derivative computed in the local equilibrium. Thus, we have

$$C(0,t) = C_0 \sin(\omega t),$$

where $C_0 = R_W q A E$ and $R_W = \frac{1}{qA}\left(\frac{d\eta}{dC}\right)_{eq}$. The conduction current $I(t)$ at $x = 0$ corresponds to the flux of diffusing particles $J(0,t)$

$$I(t) = qAJ(0,t), \tag{17}$$

where $q$ is the charge of the particle and $A$ is the area of the sample surface. The surface located at $x = L$ can be treated as fully absorbing, partially absorbing or fully reflecting wall (figure 1). Thus, the second boundary condition, fixed at the wall $x = L$, can be chosen in different ways depending on the properties of the wall. Usually, for the system described by the parabolic (sub)diffusion equation one can adopt the boundary conditions as follows:

- For the fully absorbing wall one gets [19]

$$C(L,t) = 0.$$

- For the fully reflecting wall there is [19]

$$J(L,t) = 0.$$

- For the partially absorbing wall the particle absorbed by the wall cannot return to the system and the boundary condition is given by [20, 21]

$$J(L,t) = \kappa C(L,t). \tag{18}$$

The boundary condition for the fully absorbing or fully reflecting wall was studied in majority works (see for example [9, 22]); however, the radiation boundary condition (18) was also used [15, 23, 24]. In this work we assume that the boundary condition at $x = L$ is given in a general form and is a linear combination of the flux and concentration, where the flux is delayed in time by $\tau$ with respect to the concentration. So, the boundary condition is

$$a_L J(L, t+\tau) + b_L C(L,t) = 0. \tag{19}$$

## 4. Diffusion impedance

The impedance of the electrochemical system $Z(i\omega)$ can be defined as its response to a voltage or current perturbation from a steady-state situation [22, 25]

$$Z(i\omega) = \frac{\hat{\eta}(i\omega)}{\hat{I}(i\omega)}, \tag{20}$$

where $\hat{\eta}(i\omega)$ and $\hat{I}(i\omega)$ are the Laplace transforms of the overvoltage and current perturbation, $\omega$ is the angular frequency. A plot of the real and imaginary parts of the impedance in the

complex plane (Re $Z$, $-$Im $Z$) as the angular frequency (treated as a parameter) is swept over a given range is called the Nyquist plot. From (16), (17) and (20) one obtains the relation

$$Z(\mathrm{i}\omega) = R_{\mathrm{W}} \frac{\hat{C}(0, \mathrm{i}\omega)}{\hat{J}(0, \mathrm{i}\omega)}. \tag{21}$$

The impedance of the diffusion layer is called the Warburg impedance. For the layer of the infinite thickness the impedance is defined as

$$Z(\mathrm{i}\omega) = \frac{R}{\sqrt{\mathrm{i}\omega}} = \frac{R}{\sqrt{2\omega}}(1 - \mathrm{i}), \tag{22}$$

where $R$ is the diffusion resistance. On the Nyquist plot the Warburg impedance is presented by the straight half-line with the slope angle $\pi/4$ passing through the origin of coordinates. In real systems the diffusion layer has a finite thickness. Let us assume, that the diffusion layer is bordered by planes localized at $x = 0$ and $x = L$. The perturbation of the voltage is applied to the medium at $x = 0$. The characteristic angular frequency is defined as

$$\omega_d \equiv \frac{D}{L^2}, \tag{23}$$

where $D$ is the diffusion coefficient. The frequency (23) is proportional to the inverse of the average time necessary for an ion to cross the sample thickness. When $\omega \gg \omega_d$ the size of the sample plays no role in the ion diffusion and the impedance is the Warburg impedance (22). However, for a low frequency the ions can be absorbed by the opposite wall before they change direction of their movement.

## 5. Subdiffusion impedance

We assume that the transport process is described by the generalized Cattaneo equation with the following initial conditions:

$$C(x, 0) = \left.\frac{\partial C(x, t)}{\partial t}\right|_{t=0} = 0. \tag{24}$$

Below we consider two models. First model ('model A') utilizes (5), the second one ('model B') uses (9) to describe subdiffusion in the considered system.

### *5.1. Model A*

The Laplace transform of (5) for the initial conditions (24) is

$$s\hat{C}(x, s) + \tau s^2 \hat{C}(x, s) = D_\alpha s^{1-\alpha} \frac{\partial^2 \hat{C}(x, s)}{\partial x^2}. \tag{25}$$

The general solution of equation (25) reads

$$\hat{C}(x, s) = B_1 \exp[\gamma_{\mathrm{A}}(s)x] + B_2 \exp[-\gamma_{\mathrm{A}}(s)x], \tag{26}$$

where

$$\gamma_{\mathrm{A}}(s) = \frac{s^{\alpha/2}}{\sqrt{D_\alpha}}\sqrt{1 + \tau s}. \tag{27}$$

The Laplace transform of the flux is

$$\hat{J}_{\mathrm{A}}(x, s) = -D_\alpha \frac{s^{1-\alpha}}{1 + \tau s} \frac{\mathrm{d}\hat{C}(x, s)}{\mathrm{d}x}. \tag{28}$$

Combining (19), (21) and (26)–(28) we obtain

$$Z_{\mathrm{A}}(s) = R_{\mathrm{W}} \frac{1}{\lambda_{\mathrm{A}}(s)} \left[ \frac{b_L \sinh(\gamma_{\mathrm{A}}(s)L) - a_L \lambda_{\mathrm{A}}(s) \cosh(\gamma_{\mathrm{A}}(s)L)}{b_L \cosh(\gamma_{\mathrm{A}}(s)L) - a_L \lambda_{\mathrm{A}}(s) \sinh(\gamma_{\mathrm{A}}(s)L)} \right], \tag{29}$$

where

$$\lambda_{\mathrm{A}}(s) = s^{1-\alpha/2} \sqrt{\frac{D_\alpha}{1+\tau s}}. \tag{30}$$

For the layer with infinite thickness ($L \to \infty$) the impedance (29) has the following form:

$$Z_{\mathrm{A}}(\mathrm{i}\omega) = R_{\mathrm{W}} \frac{\sqrt{1+\tau \mathrm{i}\omega}}{\sqrt{D_\alpha}(\mathrm{i}\omega)^{1-\alpha/2}}. \tag{31}$$

For $\tau = 0$ and $\alpha = 1$ equation (31) corresponds to the classical Warburg impedance [22]. For subdiffusive systems the relation on the impedance (23) should be replaced by $\omega_d \equiv (D/L^2)^{1/\alpha}$ [9].

When $\omega \to \infty$, a substantial influence of $\tau$ can be inferred from (27), (29) and (30). After calculations we obtain

- For $\tau \neq 0$

$$Z_{\mathrm{A}}(\mathrm{i}\omega) = \frac{R_{\mathrm{W}}\sqrt{\tau}}{\sqrt{D_\alpha}\omega^{(1-\alpha)/2}} \left[ \cos\left(\pi \frac{1-\alpha}{4}\right) - \mathrm{i}\sin\left(\pi \frac{1-\alpha}{4}\right) \right], \tag{32}$$

  and the Nyquist plot of the impedance is a linear function passing through the origin of coordinates with the angle slope $\phi_{\mathrm{A}}$ given by

$$\phi_{\mathrm{A}} = \pi \frac{1-\alpha}{4}. \tag{33}$$

  Let us note that for $0 < \alpha < 1$ there is $\phi_{\mathrm{A}} \in (0, \pi/4)$.

- For $\tau = 0$

$$Z_{\mathrm{A}}(\mathrm{i}\omega) = \frac{R_{\mathrm{W}}}{\sqrt{D_\alpha}\omega^{1-\alpha/2}} \left[ \cos\left(\pi \frac{1-\alpha/2}{2}\right) - \mathrm{i}\sin\left(\pi \frac{1-\alpha/2}{2}\right) \right],$$

  thus,

$$\phi_{\mathrm{A}} = \pi \frac{1-\alpha/2}{2}, \tag{34}$$

  and $\phi_{\mathrm{A}} \in (\pi/4, \pi/2)$.

For low $\omega$ one obtains

$$Z_{\mathrm{A}}(\mathrm{i}\omega) = -\frac{R_{\mathrm{W}}}{\lambda_{\mathrm{A}}(\mathrm{i}\omega)} \left[ \frac{a_L \lambda_{\mathrm{A}}(\mathrm{i}\omega) - b_L L \gamma_{\mathrm{A}}(\mathrm{i}\omega) + a_L L \lambda_{\mathrm{A}}(\mathrm{i}\omega)\gamma_{\mathrm{A}}(\mathrm{i}\omega)}{a_L \lambda_{\mathrm{A}}(\mathrm{i}\omega) + b_L L \gamma_{\mathrm{A}}(\mathrm{i}\omega) - a_L L \lambda_{\mathrm{A}}(\mathrm{i}\omega)\gamma_{\mathrm{A}}(\mathrm{i}\omega)} \right]. \tag{35}$$

An analysis of (35) leads to the following conclusions. For $\omega \to 0$ and $\alpha \in (0, 1)$ the slope of the plot is $\phi_{\mathrm{A}} = \pi(1-\alpha)/2$ when $a_L = 0$ (for the partially or fully absorbing wall) and $\phi_{\mathrm{A}} = \pi/2$ when $b_L = 0$ (for reflecting wall). We note that for $\omega \ll 1/\tau$ the terms which contain the $\tau$ parameter can be neglected in the above formulae. Then, $\phi_{\mathrm{A}}$ is independent of $\tau$.

Calculating $\mathrm{Re}\, Z$ and $\mathrm{Im}\, Z$ from (29) for $s = \mathrm{i}\omega$ we obtain the Nyquist plots (figures 2–5) with several values of the parameters $\tau$ and $\alpha$. Our calculations were done for $\omega \in (10^{-1}, 10^5)$, $R_{\mathrm{W}} = 1$, $L = 1$ and $D_\alpha = 1$ (all quantities are in arbitrary units). For larger values of $\omega$ the points on the plots are located near the origin and for larger $\tau$ the curves are located near the Re $Z$-axis.

On figures 2 and 3 the plots for $\tau = 0$ and $\tau = 0.01$ are practically undistinguishable, but for larger values of the subdiffusion parameter $\alpha$ these plots differ from each other. The

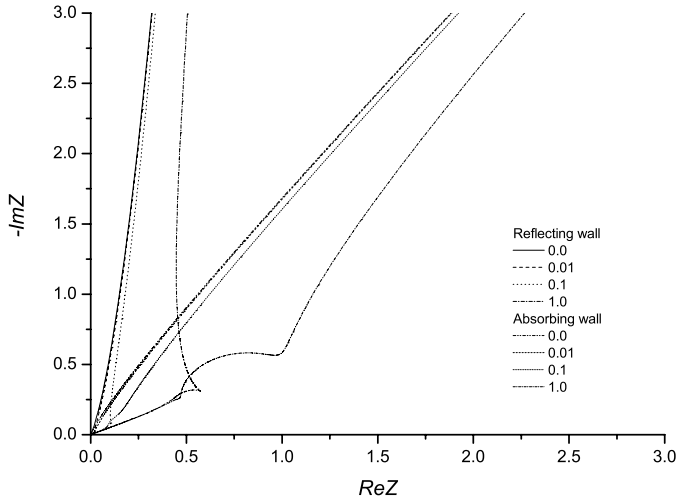


**Figure 2.** The Nyquist plots for model A with $\alpha = 0.4$ and for $\tau$ given in the legend; the additional description is in the text.

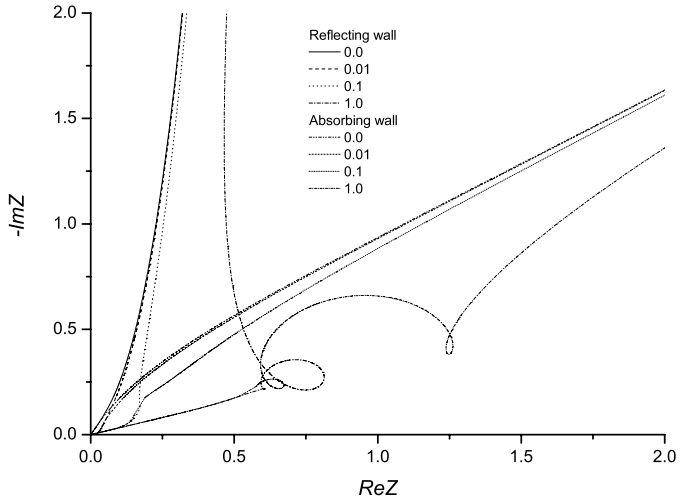


**Figure 3.** The description is the same as in figure 2 but for $\alpha = 0.6$.

plots suggest that the curves for different values of $\tau$ converge into one curve for very small values of $\omega$. For relatively large values of $\tau$ the Nyquist plots show 'chaotic' behavior, which is stronger when $\alpha$ increases. Therefore, in the presented cases we did not consider values of $\tau$ larger than that on plots in figures 2–3.

### *5.2. Model B*

The Laplace transform of (9) for the initial conditions (24) is

$$s\hat{C}(x,s) + \tau^{\alpha} s^{1+\alpha} \hat{C}(x,s) = D s^{1-\alpha} \frac{\partial^2 \hat{C}(x,s)}{\partial x^2}. \tag{36}$$

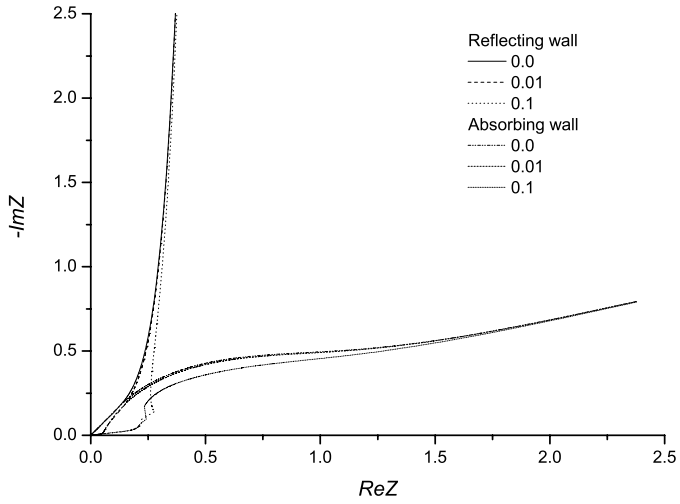


**Figure 4.** The case of model A with $\alpha = 0.8$; the further description is the same as in figure 2.

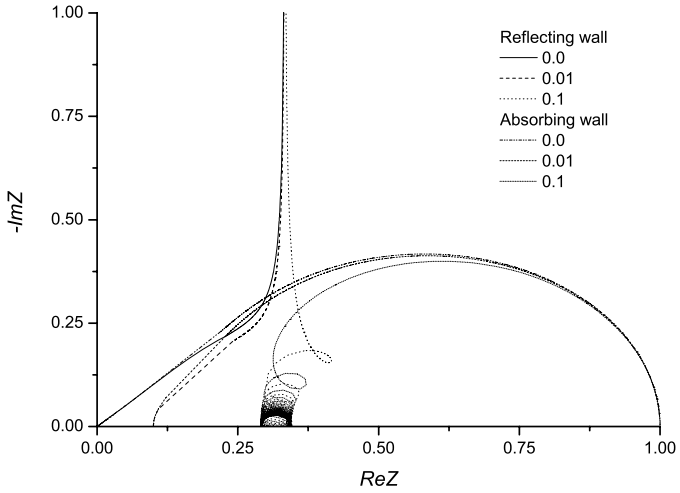


**Figure 5.** The Nyquist plots for models A and B for the normal diffusion case ($\alpha = 1.0$); the further description is the same as in figure 2.

The general solution of equation (36) reads

$$\hat{C}(x,s) = B_1 \exp[\gamma_{\mathrm{B}}(s)x] + B_2 \exp[-\gamma_{\mathrm{B}}(s)x], \tag{37}$$

where

$$\gamma_{\mathrm{B}}(s) = \frac{s^{\alpha/2}}{\sqrt{D_\alpha}}\sqrt{1+(\tau s)^\alpha}. \tag{38}$$

The Laplace transform of the flux is

$$\hat{J}_{\mathrm{B}}(x,s) = -D_\alpha \frac{s^{1-\alpha}}{1+(\tau s)^\alpha}\frac{\mathrm{d}\hat{C}(x,s)}{\mathrm{d}x}. \tag{39}$$

Combining (19), (21) and (37)–(39) we obtain

$$Z_{\mathrm{B}}(s) = R_{\mathrm{W}} \frac{1}{\lambda_{\mathrm{B}}(s)} \left[ \frac{b_L \sinh(\gamma_{\mathrm{B}}(s)L) - a_L \lambda_{\mathrm{B}}(s) \cosh(\gamma_{\mathrm{B}}(s)L)}{b_L \cosh(\gamma_{\mathrm{B}}(s)L) - a_L \lambda_{\mathrm{B}}(s) \sinh(\gamma_{\mathrm{B}}(s)L)} \right], \tag{40}$$

where

$$\lambda_{\mathrm{B}}(s) = s^{1-\alpha/2} \sqrt{\frac{D_\alpha}{1+(\tau s)^\alpha}}. \tag{41}$$

For the layer with the infinite thickness ($L \to \infty$) the impedance (40) has the following form:

$$Z_{\mathrm{B}}(\mathrm{i}\omega) = R_{\mathrm{W}} \frac{\sqrt{1+(\mathrm{i}\omega\tau)^\alpha}}{\sqrt{D_\alpha}(\mathrm{i}\omega)^{1-\alpha/2}},$$

which for $\alpha = 1$ is identical with $Z_{\mathrm{A}}(\mathrm{i}\omega)$ (see (31)).

When $\omega \to \infty$ from (38), (40) and (41) we obtain

- For $\tau \neq 0$

$$Z_{\mathrm{B}}(\mathrm{i}\omega) = \frac{R_{\mathrm{W}}}{\omega^{1-\alpha}} \sqrt{\frac{\tau^\alpha}{D_\alpha}} \left[ \cos\left(\pi \frac{1-\alpha}{2}\right) - \mathrm{i} \sin\left(\pi \frac{1-\alpha}{2}\right) \right], \tag{42}$$

  and the Nyquist plot of the impedance is a linear function passing through the origin of coordinates with the angle slope $\phi_{\mathrm{B}}$ given by

$$\phi_{\mathrm{B}} = \pi \frac{1-\alpha}{2}, \tag{43}$$

  thus, for $0 < \alpha < 1$ there is $\phi_{\mathrm{B}} \in (0, \pi/2)$.

- For $\tau = 0$

$$Z_{\mathrm{B}}(\mathrm{i}\omega) = \frac{R_{\mathrm{W}}}{\sqrt{D_\alpha}\omega^{1-\alpha/2}} \left[ \cos\left(\pi \frac{1-\alpha/2}{2}\right) - \mathrm{i} \sin\left(\pi \frac{1-\alpha/2}{2}\right) \right],$$

  so,

$$\phi_{\mathrm{B}} = \pi \frac{1-\alpha/2}{2}, \tag{44}$$

  and $\phi_{\mathrm{B}} \in (\pi/4, \pi/2)$.

  For low $\omega$ one obtains

$$Z_{\mathrm{B}}(\mathrm{i}\omega) = -\frac{R_{\mathrm{W}}}{\lambda_{\mathrm{B}}(\mathrm{i}\omega)} \left[ \frac{a_L \lambda_{\mathrm{B}}(\mathrm{i}\omega) - b_L L \gamma_{\mathrm{B}}(\mathrm{i}\omega) + a_L L \lambda_{\mathrm{B}}(\mathrm{i}\omega)\gamma_{\mathrm{B}}(\mathrm{i}\omega)}{a_L \lambda_{\mathrm{B}}(\mathrm{i}\omega) + b_L L \gamma_{\mathrm{B}}(\mathrm{i}\omega) - a_L L \lambda_{\mathrm{B}}(\mathrm{i}\omega)\gamma_{\mathrm{B}}(\mathrm{i}\omega)} \right]. \tag{45}$$

An analysis of (45) leads to the following conclusions. For $\omega \to 0$ and $\alpha \in (0, 1)$, the slope of the plot is $\phi_{\mathrm{B}} = \pi(1-\alpha)/2$ when $a_L = 0$ (for the partially or fully absorbing wall) and $\phi_{\mathrm{B}} = (1-3\alpha/4)\pi$ when $b_L = 0$ (for reflecting wall). Similarly as in the model A, $\phi_B$ is independent of $\tau$.

The Nyquist plots obtained from (40) are presented in figures 6–8 for several values of the parameters $\tau$ and $\alpha$, where $\omega \in (10^{-1}, 10^5)$, $R_{\mathrm{W}} = 1$, $L = 1$ and $D_\alpha = 1$ (all quantities are in arbitrary units). We add that for the case of $\alpha = 1$ as well as for $\tau = 0$ the plots obtained from model A and model B are identical to each other.

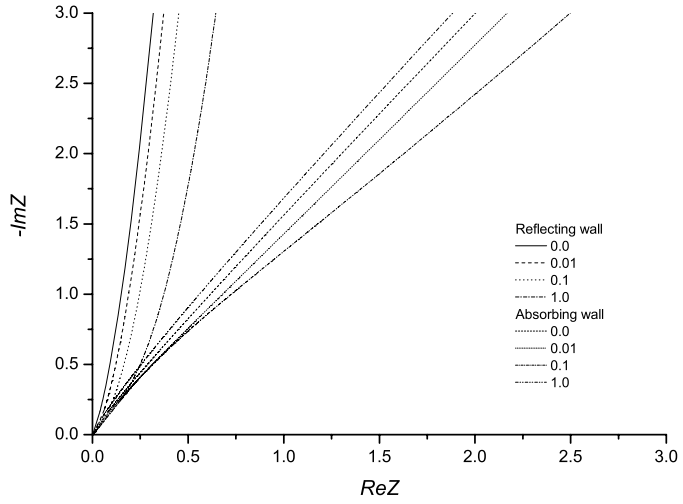


**Figure 6.** The Nyquist plots for model B with $\alpha = 0.4$ and for $\tau$ given in the legend; the additional description is in the text.

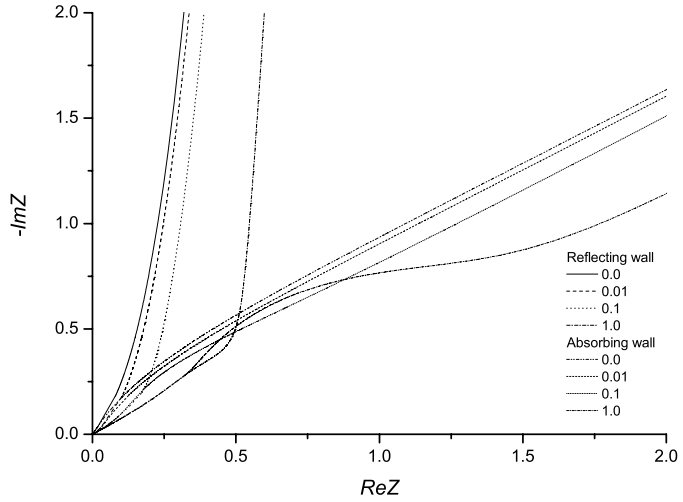


**Figure 7.** The description is the same as in figure 6 but for $\alpha = 0.6$.

## 6. Final remarks

In our paper we consider two models of subdiffusive impedance, where the different hyperbolic subdiffusion equations were taken into consideration. These equations are not equivalent to each other and they have different physical meaning. Consequently, the subdiffusive impedance formulae derived from these equations are not equivalent to each other as well.

The main results of our paper are equation (29) with the asymptotic formulae (32)–(35) for model A and equation (40) with the asymptotic formulae (42)–(45) for model B. These functions illustrated by the plots (figures 2–5) for model A and 5–8 for model B show the following.

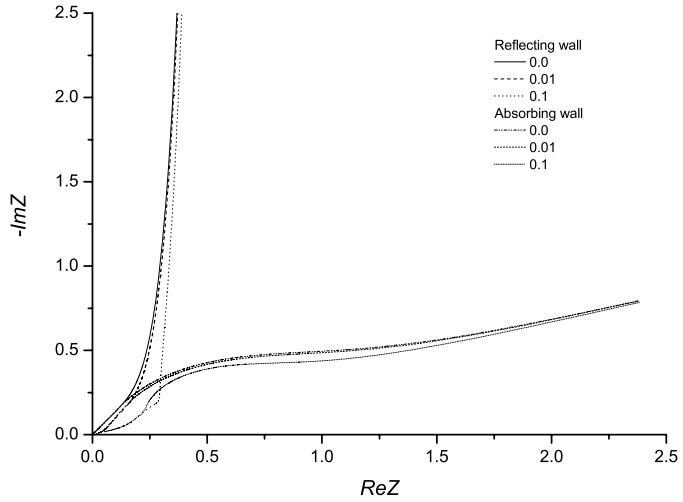


**Figure 8.** The Nyquist plots for model B with $\alpha = 0.8$; the further description is the same as in figure 6.

For $\omega \to \infty$ the Nyquist plot is the linear function passing through the origin of coordinates with the slope angle $\phi_A$ and $\phi_B$, respectively, depending on the subdiffusion parameter $\alpha$ and given by (33) and (34) for model A and by (43) and (44) for model B. It is interesting that both $\phi_A$ and $\phi_B$ do not depend on the parameter $\tau$ explicitly, but the dependence is 'hidden' and is manifested by the interval to which the parameter belongs. For a given $\alpha \in (0, 1)$ and $\tau \neq 0$ $\phi_A = \pi(1-\alpha)/4 < \pi/4$ and $\phi_B = \pi(1-\alpha)/2 < \pi/2$, so, $\phi_B = 2\phi_A$ (see figure 9). For non-zero $\tau$, $\phi_A$ as well as $\phi_B$ do not depend on $\tau$ and for all values of $\phi_A$ and $\phi_B$ they are independent of the boundary conditions at $x = L$. For a given $\alpha \in (0, 1)$ and $\tau = 0$ $\phi_A = \pi(1-\alpha/2)/2 > \pi/4$ and $\phi_B = \pi(1-\alpha/2)/2 > \pi/4$. In this case $\phi_A = \phi_B$. In this paper [24] the case of $\phi \neq \pi/4$ was interpreted somewhat differently, mainly as a presence of so-called 'constant phase element' (CPE) in the system.

For relatively high $\omega$ and for $\tau \neq 0$ the Nyquist plots for both models show the 'chaotic' and 'oscillating' behavior, increasing with the increased $\tau$ and $\alpha$ parameters. The physical interpretation of this fact can be as follows. Namely, the periodic changes of the concentration at the surface $x = 0$ generated the flux which is delayed in time by $\tau$ with respect to the concentration gradient. When the oscillations of the concentration are very rapid, the flux does not keep up with the concentration changes, so the additional factor contributing to the total impedance is created. The difficulties in movement of the ions increase when $\alpha$ decreases causing a decrease in the flux. Thus, the parameter $\tau$ influences the transport process less when $\alpha$ is smaller. Such a behavior is observed on the presented plots, where the curves obtained for $\tau = 0$ and for $\tau = 0.1$ differ slightly from each other when $\alpha = 0.4$ and $\alpha = 0.6$, but the difference is relatively large for $\alpha = 0.8$ and $\alpha = 1$. The 'chaotic' behavior for model B is clearly smaller than for model A (see figures 2 and 6 or 3 and 7 or 4 and 8).

For low $\omega$ the plots are dependent on the boundary conditions. According to (35) and (45), for fully reflecting wall and for $\omega \ll 1/\tau$ one gets $\phi_A = \pi/2$ for all values of $\alpha$ and $\phi_B = (1 - 3\alpha/4)\pi$. For fully or partially permeable wall we observe that the plots for model A as well as for model B become linear with $\phi_{A,B} = \pi(1-\alpha)/2$.

As we mentioned in the introduction, there are a few methods for extracting the value of subdiffusion parameter from experimental data. The considerations presented in this paper

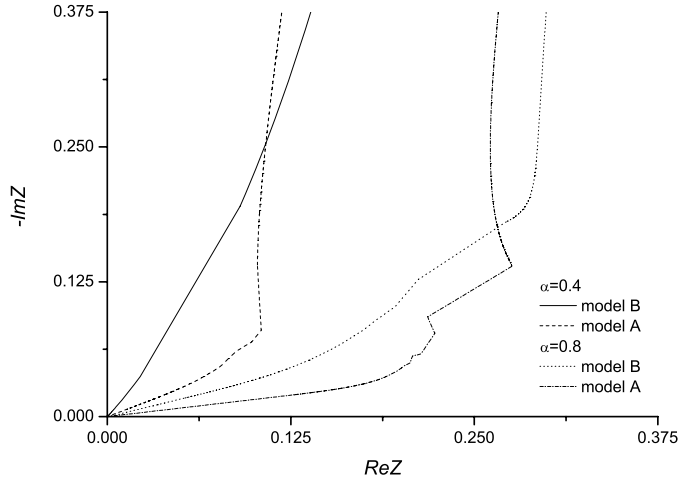


**Figure 9.** The comparison between models A and B for the subdiffusion parameters $\alpha$ given in the legend, with $\tau = 0.1$.

show that it is possible to determine the value of parameter of the system from the Nyquist plots obtained experimentally. However, model A and model B give quite different results. It seems that there is no experimental basis to judge which model should be used. On the basis of our theoretical considerations we declare for model A because of the following reasons:

- as we discussed in section 2 the microscopic model B does not lead to the parabolic subdiffusion equation with the infinity speed of propagation,
- in model B parameters $D_\alpha$ and $\tau$ are related to each other whereas in other formalisms leading to the hyperbolic subdiffusion equation (see e.g. [26, 27]) these parameters are treated as independent of each other.

The model A is free from the above objections. So, to extract the subdiffusion parameter from the experimental data we use model A. In [8] there was studied lithium transport through vanadium pentoxide xerogel film electrode. The authors found that $\phi = 32^\circ$, it was interpreted the results as the subdiffusive transport of the particles inside the electrode. Since $\phi < 45^\circ$, we deduce that the transport studied in [8] can be described by the Cattaneo equation with non-zero parameter $\tau$ and with $\alpha = 0.38$ (see (33)). Unfortunately, the value of the slope angle is not sufficient to extract $\tau$ from experimental data. To find this parameter one should perform more detailed studies where the parameter representation of the Nyquist plots is taken into consideration.

For the system described by the parabolic subdiffusion equation (1) we obtain $\phi > \pi/4$, whereas $\phi < \pi/4$ corresponds to the model with non-zero $\tau$. We add that, to achieve the latter situation, the subdiffusion equation different from (1) was included into the impedance model [9]. Namely, it was assumed that the subdiffusion is described by one of the following equations:

$$\frac{\partial^\alpha C(x,t)}{\partial t^\alpha} = D_\alpha \frac{\partial^2 C(x,t)}{\partial x^2}, \tag{46}$$

$$\frac{\partial^{2-\alpha} C(x,t)}{\partial t^{2-\alpha}} = D_\alpha \frac{\partial^2 C(x,t)}{\partial x^2}, \tag{47}$$

when both of the equations contain the Riemann–Liouville fractional derivative. However, physical meaning of equations (46) and (47) is rather unknown since they were derived only in a phenomenological way, where the time derivative of natural order was replaced by the fractional one in the continuity equation and/or in the Fick's law. These equations were not derived on the basis of a 'microscopic' model such as the continuous time random walk formalism. We note that (1) is equivalent to (46) if in the latter one the Riemann–Liouville fractional derivative is replaced by the Caputo derivative. In our paper we show that the slope $\phi < \pi/4$ is achieved from the model based on the hyperbolic subdiffusion equation.

## Acknowledgments

This paper was partially supported by Polish Ministry of Education and Science under grant no. 1 P03B 136 30.

## References

[1] Metzler R and Klafter J 2000 *Phys. Rep.* **339** 1–77
Metzler R and Klafter J 2004 *J. Phys. A: Math. Gen.* **37** R161–208
[2] Kosztołowicz T, Dworecki K and Mrówczyński S 2005 *Phys. Rev. Lett.* **94** 170602
Kosztołowicz T, Dworecki K and Mrówczyński S 2005 *Phys. Rev.* E **71** 041105
[3] Bisquert J *et al* 2000 *J. Phys. Chem.* B **104** 2287
[4] Diaz B, Novoa X R and Perez M C 2006 *Cem. Concr. Compos.* **28** 237
[5] Cabeza M *et al* 2002 *Cem. Concr. Compos.* **32** 881
[6] Cabeza M *et al* 2006 *Electrochim. Acta* **51** 1831
[7] Reyes-Gasga J *et al* 1999 *J. Mater. Sci.* **34** 2183
[8] Jung K N, Pyun S I and Lee J W 2004 *Electrochim. Acta* **49** 4371–8
[9] Bisquert J and Compte A 2001 *J. Electroanal. Chem.* **499** 112–20
[10] Oldham K B and Spanier J 1974 *The Fractional Calculus* (New York: Academic)
[11] Podlubny I 1999 *Fractional Differential Equations* (San Diego: Academic)
[12] Cattaneo G 1948 *Atti Semin. Mat. Fis. Univ. Modena* **3** 83–101
[13] Compte A and Metzler R 1997 *J. Phys. A: Math. Gen.* **30** 7277–89
[14] Kosztołowicz T, Lewandowska K D and Głogowska B 2008 arXiv:0806.2294
[15] Criado C, Galan–Montenegro V, Velasquez P and Ramos–Barrado J R 2000 *J. Electroanal. Chem.* **488** 59
[16] Ramos–Barrado J R, Galan Montenegro P and Criado Cambon C 1996 *J. Chem. Phys.* **105** 2813–15
[17] Lewandowska K D and Kosztołowicz T 2008 *Acta Phys. Pol.* B **39** 1211–20
[18] Freger V 2005 *Electrochem. Commun.* **7** 957
[19] Chandrasekhar S 1943 *Rev. Mod. Phys.* **15** 1–89
[20] Razi Naqvi K, Mork K J and Waldenstrom S 1982 *Phys. Rev. Lett.* **49** 304
[21] Kosztołowicz T 2001 *Physica* A **298** 285–96
[22] Ross Macdonald J 1987 *Impedance Spectroscopy* (New York: Wiley)
[23] Diard J P, Le Gorrec B and Montella C 1999 *J. Electroanal. Chem.* **471** 126
[24] Bisquert J, Garcia-Belmonte G, Bueno P R, Longo E and Bulhoes L O S 1998 *J. Electroanal. Chem.* **452** 229
[25] Jacobsen T and West K 1995 *Electrochim. Acta* **40** 255
[26] Kubo R, Toda M and Hashitsume N 1985 *Statistical Physics* (Berlin: Springer)
[27] Jou D, Casas–Vazquez J and Lebon G 2000 *Extended Irreversible Thermodynamics* (Berlin: Springer)